

Resveratrol inhibits paclitaxel-induced neuropathic pain by the activation of PI3K/Akt and SIRT1/PGC1 α pathway

Xiaoning Li¹
Shuhong Yang¹
Liang Wang¹
Peng Liu¹
Shuang Zhao¹
Huizhou Li¹
Yuqing Jiang²
Yuexian Guo²
Xiuli Wang¹

¹Department of Anesthesiology, The Third Hospital of Hebei Medical University, Qiaoxi District, Shijiazhuang 050051, China;

²Department of Urology, The Third Hospital of Hebei Medical University, Qiaoxi District, Shijiazhuang 050051, China

Background: Phosphoinositide 3-kinase (PI3K)/protein kinase B (Akt) is one of the essential signaling pathways for the development and maintenance of neuropathic pain.

Objective: To investigate the effect of resveratrol (RES) on paclitaxel-induced neuropathic pain in rats and elucidate the underlying molecular mechanisms.

Method: Male Sprague Dawley rats were randomly divided into seven groups (n=10/group): Group C, Group P, Group R, Group R+P, Group LY + R+P, Group LY (the specific inhibitor of PI3K), Group E (the specific inhibitor of sirtuin 1 [SIRT1]). Paw withdrawal mechanical threshold (PWT) and thermal withdrawal latency (TWL) were recorded. Mitochondrial histomorphology was performed by transmission electron microscope. PI3K, p-Akt, and t-Akt expressions were tested using immunohistochemistry. Western blot was used to detect p-Akt, t-Akt, SIRT1, and PGC1 α expressions. The apoptosis in the striatum, spinal dorsal horns (SDH), and dorsal root ganglions (DRG) tissues was assayed by TUNEL. ELISA was used to detect the contents of IL- β , IL-10, malondialdehyde (MDA), and superoxide dismutase (SOD) in striatum, SDH, and DRG tissues.

Results: Compared to the control group, PWT and TWL in the P and LY +R+P groups were significantly decreased on 8th and 14th day after paclitaxel administration ($P<0.05$). The expressions of p-Akt, SIRT1, and PGC1 α were decreased in paclitaxel-induced neuropathic rats; however, the expressions of p-Akt, SIRT1, and PGC1 α were significantly increased after RES treatment ($P<0.05$). Furthermore, the expression of p-Akt was decreased by LY294002 ($P<0.05$), and amount of SIRT1 and PGC1 α expression was inhibited by EX-527 ($P<0.05$). The t-Akt level was not significantly changed in all groups. RES prevented paclitaxel-induced mitochondrial damage by PI3K/Akt. RES improves the pain symptoms of paclitaxel neuralgia rats by increasing the IL-10 and decreasing the expression of IL-1 β . RES increases the SOD and reduces the MDA. RES reduces apoptosis by SIRT1/PGC1 α signal pathway.

Conclusion: Our results suggest that RES may inhibit paclitaxel-induced neuropathic pain via PI3K/Akt and SIRT1/PGC1 α pathways.

Keywords: resveratrol, paclitaxel, neuropathic pain, PI3K/Akt, SIRT1/PGC1 α

Introduction

Peripheral neuropathy caused by chronic, distal, and symmetrical chemotherapy, commonly accompanied by a neuropathic pain syndrome, is a serious dose-limiting complication associated with several first-line chemotherapeutic agents.²⁶ Paclitaxel (Taxol[®]) has long been established as a preferred chemotherapeutic agent for the treatment of solid tumors in clinical practices.^{10,14} Paclitaxel-induced neuropathic pain is characterized by hypersensitivity to mechanical and cold stimuli that develop early

Correspondence: Xiuli Wang
Department of Anesthesiology, The Third Hospital of Hebei Medical University, No. 139, Ziqiang Road, Qiaoxi District, Shijiazhuang 050051, China
Tel +86 185 3311 2928
Email wangxl301@yeah.net

at the initiation of treatment, and it even persists for weeks or years after termination of treatment.¹¹ Long-term neuropathic pain is considered to be associated with decreasing the patients' quality of life³¹ and restricting optimal dosage.⁵ However, the prevention and treatment of paclitaxel-induced neuropathic pain are limited owing to the poor knowledge of its molecular mechanisms. Previous studies have revealed that paclitaxel-induced painful peripheral neuropathies were associated with an abnormal incidence of swollen and vacuolated mitochondria in peripheral sensory nerve axons.^{5,13} In addition, a number of researches have demonstrated that accumulation of ROS could induce oxidative stress, leading to neuronal cytotoxicity and mitochondrial dysfunction,^{3,29} which plays an important role in the pathogenesis of neuronal damage and degeneration. Thus, mitochondria function in peripheral nerve from chemotherapy-treated animals may be a potential target for the treatment of neuropathic pain, and it needs a clear test for this hypothesis. In the current study we observe that paclitaxel-induced neuropathic pain causes the damage of hippocampal cells in the brain. Furthermore, paclitaxel-induced neuropathic pain has not only effect on spinal dorsal horns (SDH) and dorsal root ganglions (DRG), but also has an effect on brain. In addition, paclitaxel-induced neuropathic pain causes the striatum mitochondrial damage in rats, while the striatum is an important central point of control. Thus, we chose SDH, DRG, as well as striatum for further study in this research. Previous study has demonstrated that mitochondrial damage of the striatum in rats with paclitaxel-induced neuropathic was serious, and the SIRT 1/PGC1 α signal pathway was closely related to mitochondrial damage.^{17,34} PGC1 α is an important regulator of mitochondrial production and oxygen free radical inhibitor.¹⁸ Malondialdehyde (MDA) and superoxide dismutase (SOD) were measured in this research in order to observe the effect of SIRT 1/PGC1 α on oxygen free radicals. On account of resveratrol (RES) having the anti-inflammatory effect,⁷ IL- β and IL-10 were measured in order to study intensively whether the rats with paclitaxel-induced neuropathic were related to release of inflammatory factors. RES is a natural phenolic antioxidant, which is commonly abundant in a variety of food sources.¹⁵ It has been reported that RES has anti-inflammatory⁹ and neuroprotective properties¹⁶ and other important therapeutic activities.²² RES is a natural agonist of sirtuin 1 (SIRT1), and the neuroprotective effect of RES is being recognized due to the direct oxidation resistance of this compound. SIRT1, a histone deacetylase, interacts with multiple proteins and participates in the process of apoptosis of cells under oxidative stress conditions. Thus, SIRT1 has

the function of protecting nerve cells. It has been reported that RES relieves neuropathic pain through the activation of spinal SIRT1.³⁴ The phosphatidylinositol 3-kinase/protein kinase B (PI3K/Akt) pathway is one of the most important participants in modulating nociceptive information and is centrally sensitized in the microglial intracellular signaling cascades.²⁵ RES has been found to protect neuronal cells from oxidative cytotoxicity via PI3K/Akt pathway.²⁴ However, the potential mechanism of RES in preventing paclitaxel-induced neuropathic pain has yet to be explored. Therefore, in this study, a rat model of paclitaxel-induced neuropathic pain was established to investigate the effect of RES on paclitaxel-induced neuropathic pain and the role of PI3K/Akt and SIRT1/PGC1 α signal pathway in relieving neuropathic pain.

Materials and methods

Experimental animals

Adult male SD rats (180–200 g) provided by the Experimental Animal Center (Hebei Medical University, Shijiazhuang, China) were housed in plastic cages under a 12-hour light/dark cycle at a temperature of 25°C with food and water available ad libitum. In addition, they were adapted to the environment at least 7 days before the experiments. All experiment procedures were performed in accordance with the guidelines of the International Association for the Study of Pain.⁶ The study was approved by the Institutional Animal Care and Use Committee of the Third Hospital of Hebei Medical University (no. 2016022).

Intrathecal catheter implantation

Rats were intraperitoneally (i.p.) injected with 1% pentobarbital sodium, a 2–3 cm longitudinal skin incision was made over L4–L5 lumbar vertebrae, and paravertebral muscles were bluntly separated. The PE-10 catheter filled with heparin saline was inserted into the subarachnoid space through the incision in the cisternal membrane and advanced 1.2 cm caudally to ensure that the tip of each catheter was positioned at the lumbar spinal level.²⁸ The final catheter location was verified by transient paralysis of the hindlimbs produced by the intrathecal injection of 5 μ L of 2% lidocaine. Rats with paralysis, catheter loss, and infection, and those that were dead were excluded. The rats with successful intrathecal catheter implantation were allowed to recover for 3–5 days before drug injection.

Drug administration

Rats were randomly divided into seven groups (n=10/group): Group C was the control rats; Group P was treated with paclitaxel (Taxol; TCI, Japan); Group R was treated

with RES (TCI); Group R+P was treated with paclitaxel and pretreated with RES; Group LY +R+P was pretreated with RES and LY294002 (2-(4-morpholinyl)-8-phenyl-4H-1-benzopyran-4-one) (Cayman, USA), followed by treatment with paclitaxel; Group LY was pretreated with RES and paclitaxel. Group E was pretreated with RES and paclitaxel, followed by treatment with EX-527 (6-chloro-2,3,4,9-tetrahydro-1H-carbazole-1-carboxamide) (MCE, USA). To induce painful neuropathy, paclitaxel was diluted with saline to a concentration of 1 mg/mL, and injected i.p. at 2 mg/kg on four alternate days (days 1, 3, 5, and 7, Figure 1) for a cumulative dose of 8 mg/kg.³³ Control rats received an equivalent volume of the vehicle (Cremophor EL/ethanol, 1:1) on the same four alternate days. RES (TCI) was prepared in 5% sodium carboxymethylcellulose to a concentration of 8 mg/mL and injected i.p. at 40 mg/mL on seven alternate days (days 2, 4, 6, 8, 10, 12, and 14, Figure 1).¹² Rats were pretreated intrathecally (i.t.) with PI3K inhibitor, LY294002 (at 2.5 µg/10 µL) on seven alternate days (Days 2, 4, 6, 8, 10, 12, and 14, Figure 1) before the addition of paclitaxel and RES.¹ The last group of rats were pretreated i.t. with SIRT1 inhibitor, EX-527 (at 10 µg/10 µL) for 14 days (Figure 1) before the addition of paclitaxel and RES.

Behavioral assays

Behavioral testing was done at the point T0 (0 day before chemotherapy), T1 (8 days after chemotherapy), and T2 (14 days after chemotherapy), respectively. The behavioral testing was performed in a fixed time point (8:00 am–12:00 pm) during the day. For mechano-allodynia assessment, rats were

placed in individual plastic boxes with a metal mesh floor and allowed to acclimate for 15 minutes before measuring the mechanical paw withdrawal thresholds (PWT) in grams by using calibrated von Frey filaments (Stoelting, WoodDale, USA, ranging from 2 to 26 × g bending force).⁴ The monofilaments were applied to the plantar surface perpendicularly, which showed the sufficient force to bend against the hind paws for 6–8 seconds. The interval time between contiguous stimuli was several seconds. Sharp paw withdrawal or paw licking was considered as a positive response. The 50% withdrawal response was calculated according to the “up-down method” of Dixon.⁸

Thermal withdrawal latency (TWL) of the hind paws was measured using the method described by Polomano.³³ The mid-plantar left hind paws of the rats were aimed by a light source in a plastic compartment atop a glass floor. The intensity of the light was adjusted at the beginning of the test such that the average baseline latency was 7 seconds with a cutoff latency of 20 seconds. Sharp paw withdrawal or paw licking was considered as a positive response. The latency of each hind paw 10 minutes apart was assessed four times, and the first measurement per side was discarded due to it being anomalously long. There was no difference between the left and right paws, and the rat’s score was the average of the four bilateral latencies.

Transmission electron microscopy

The rats were anesthetized with 1% sodium pentobarbital and killed at day 15 following paclitaxel-induced neuropathic pain. The striatum from the rats was fixed in 2% paraformal-

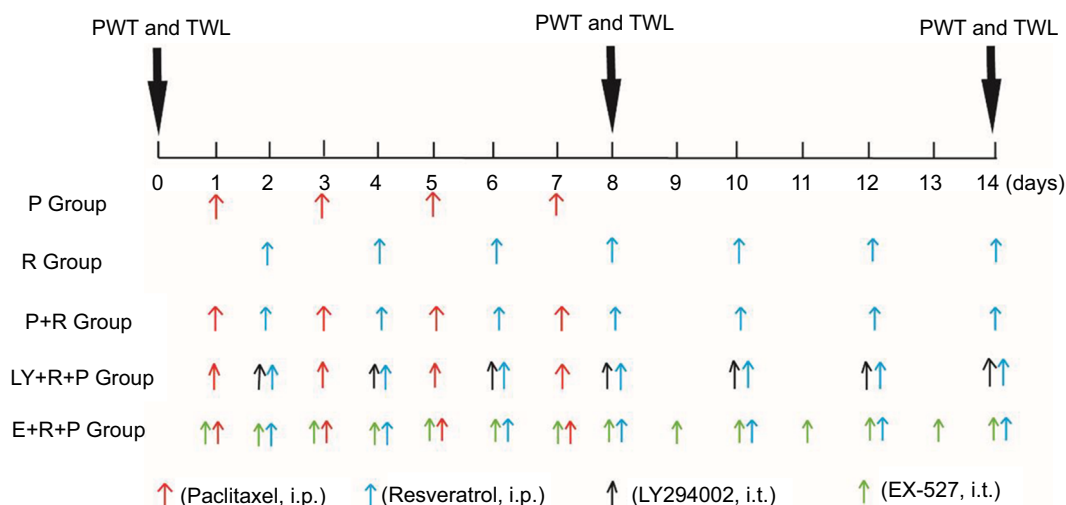


Figure 1 Schematic of the experimental process. i.p. stands for injected intraperitoneally; i.t. stands for intrathecally.

Abbreviations: i.p., intraperitoneally; i.t., intrathecally; PWT, paw withdrawal mechanical threshold; TWL, thermal withdrawal latency.

dehyde plus 2% glutaraldehyde (pH 7.4) for 2 hours, and then was sectioned ($1 \times 1 \times 1 \text{ mm}^3$). Postfixed tissue was incubated in 1% osmium tetroxide (0.1 M, pH 7.4) and dehydrated in ascending concentrations of ethanol and acetone at room temperature, then embedded in resin. Ultrathin sections (60 nm) were obtained using an ultramicrotome (UC-7; Leica, Germany) and then stained with lead citrate and uranyl acetate. Samples were detected using transmission electron microscope (H-7500; Hitachi, Japan) for analysis at 15,000 \times magnifications.

Immunohistochemistry

p-Akt, t-Akt, and PI3K expressions were analyzed for each group. The striatum was fixed in 4% paraformaldehyde, and then it was set into paraffin blocks for sectioning on a microtome of 5 μm thickness and mounted on polylysine slides. Then deparaffinization and rehydration in graded ethanol concentrations were performed, followed by suitable antigen retrieval in 0.01 M citrate buffer (pH 6.0) by microwaving. Endogenous peroxidase was blocked by 3% hydrogen peroxide (H_2O_2) for 15–20 minutes. Nonspecific antibody binding sites were blocked with 5% goat serum in 0.01 M PBS for 20 minutes. Then, the sections were incubated with primary antibodies (Boster, Wuhan, China) against p-Akt (BM4721, 1:100), t-Akt (BM4390, 1:100), and PI3K (BM4371, 1:100) overnight. Subsequently, these sections were processed with secondary antibody IgG (sp-9002; ZSGB-BIO, Beijing, China sp-9002) for 20 minutes. Thereafter, the slides were incubated with horseradish peroxidase (HRP)-labeled streptomycin (zli-9032; ZSGB-BIO) for 20 minutes. Immunodetection was done using Diaminobenzidine (DAB) as chromogen and H_2O_2 as substrate, followed by counter-staining with hematoxylin. After immunohistochemistry, images (400 \times) were captured randomly. Image-Pro Plus 6.0 (Media Cybernetics, MD, USA) was used to analyze the change in the average OD of p-Akt, t-Akt, and PI3K. The immunohistochemical score (IHS) was evaluated semiquantitatively and scored as follows: no staining is scored as 0, 1%–10% of cells stained scored as 1, 11%–50% as 2, 51%–80% as 3, and 81%–100% as 4. Staining intensity is rated on a scale of 0–3, with 0= negative; 1= weak; 2= moderate, and 3= strong. Theoretically, the scores could range from 0 to 12. An IHS of 9–12 was considered strong immunoreactivity, 5–8 was considered moderate, 1–4 was considered weak, and 0 was expected as negative.

Western blot analysis

The levels of t-Akt, p-Akt, SIRT1, and PGC1 α were determined by Western blot analysis, with β -actin as internal

reference protein. The fresh striatum, SDH, and DRG were washed with ice-cold PBS and immersed in 100 μL of lithium dodecyl sulfate sample buffer (Novex, USA) containing 1% protease inhibitor. Total protein concentrations were determined with a modified bicinchoninic acid assay (Beyotime, China). Proteins were separated by electrophoresis on 12% SDS-PAGE gels. Separated proteins were transferred onto polyvinylidene difluoride membrane (Merk Millipore, Billerica, MA, USA). The membrane was blocked for 2 hours at room temperature with 5% nonfat dry milk in TBS buffer (50 mM Tris-HCl, pH 7.5, 150 mM NaCl) containing 0.1% Tween-20 (TBST), and then incubated with primary antibodies against monoclonal rabbit Akt (1:1000; Cell Signaling Technology, USA) and monoclonal rabbit p-Akt (1:1000; Cell Signaling Technology) for 2 hours at room temperature. After washing with TBST, the membranes were incubated for 2 hours at room temperature with a secondary anti-rabbit antibody conjugated to HRP (KPL, USA) and developed using the enhanced chemiluminescence system (GE Healthcare, Canada). Negative controls did not contain primary antibody. The relative ODs of the specific bands visible on X-ray film were scanned and measured by image analysis software (BandScan 5.0).

The TUNEL assay

During the 15 days of experiment, 5 rats in each group were randomly selected and i.p. injected with 1% sodium pentobarbital at a dose of 40 mg/kg. Rats were placed in the supine position, and the chest was dissected to expose the heart. The perfusion needle was inserted from the apex to the left ventricle and fixed by hemostatic forceps, and the right atrial appendage was cut to form a perfusion channel. The left ventricle was rapidly perfused with 37 $^\circ\text{C}$ normal saline and then drained through the right atrial appendage. Rats' limbs, liver, and intestines were observed when clear normal saline was drained out from the right atrial appendage. The perfusate was replaced normal saline to 4% paraformaldehyde when the liver turns pale and the intestines become swollen. Air should not be present during operation. When the rat limbs were suddenly stressed and the tail was curled, the perfusion speed lowered. The total amount of 4% paraformaldehyde was about 300 mL. After perfusion was completed, corpus striatum, SDH, and DRG were rapidly removed and stored in 4% paraformaldehyde. After paraffin embedding and tissue sectioning (4 μm thickness), deparaffinization and rehydration were performed in graded ethanol concentrations. Endogenous peroxidase was blocked by 3% hydrogen peroxide (H_2O_2) for 10–15 minutes. Slides were

incubated for 15–30 minutes with Proteinase K (20 µg/mL in Tris/HCl, pH 7.4–8.0) at 37°C. Slides were washed two times with PBS (5 minutes in each), and incubated in 50 µL TUNEL reaction mixture for 1 hour at 37°C in a dark and humidified box. Slides after three washes with PBS (5 minutes in each) were incubated in 50 µL transformant-POD for 30 minutes at 37°C in a dark and humidified box. Slides were washed five times with PBS (5 minutes in each) and each slide was covered with 50–100 µL DAB substrate solution and incubated for 5–10 minutes at room temperature. Then, each slide was covered with 50 µL hematoxylin for 5 minutes to counterstain the nuclei. The images were acquired using a conventional microscope.

The assay of ELISA

The fresh striatum, SDH, and DRG tissues were washed with precooled PBS to remove residual blood, and then weighed it. The tissue and PBS were added to a glass homogenizer in a weight ratio of 1:9 (1 g:9 mL) and homogenated on ice. Finally, the well-mixed homogenate was centrifuged for 5–10 minutes at 5000 rpm, and the supernatant was taken for detection according to the specific steps of IL-1 β (ELISA, mlbio), IL-10 (ELISA, mlbio), MDA (ELISA, mlbio), and SOD (ELISA, mlbio) as per the manufacturer's instructions.

Statistical analysis

Statistical analysis was performed by using SPSS (version 21.0, Inc., Chicago, IL, USA). The measurement data are presented as mean \pm SD and analyzed by one-way ANOVA, followed by a Student–Newman–Keuls multiple comparison test. *P* values <0.05 were considered statistically significant.

Results

Effects of RES and LY294002 on paclitaxel-induced neuropathic pain

The mice received paclitaxel at days 1, 3, 5, and 7. The mechanical allodynia and heat hypersensitivity were tested at T0 (0 day before paclitaxel administration), T1 (8 days after paclitaxel administration), and T2 (14 days after paclitaxel administration), respectively. Compared to the control group at T1 and T2, the PWT and TWL were significantly decreased in the groups P and LY (*P*<0.05). Compared to group P at T1 and T2, PWT and TWT were significantly increased in P+R group (*P*<0.05). However, PWT and TWT were not significantly changed in the groups C and R (Figure 2A and B). The results revealed that paclitaxel could efficiently induce the mechanical and heat hypersensitivity.

Transmission electron microscopy observation in mitochondria

As shown in Figure 2, the mitochondrial histomorphology in the corpus striatum of five groups at day 14 was observed by transmission electron microscopy. The structure of mitochondria was found to be normal in the control and RES groups (Figure 3A and B). The incidences of swollen and vacuolated mitochondria were observed in the paclitaxel-treated group (Figure 3C). Paclitaxel-induced mitochondrial damage was attenuated by RES treatment (Figure 3D). Furthermore, in the LY + R+P group, swollen and vacuolated mitochondria were found to be worsened (Figure 3E).

Immunoreactivity of p-Akt, t-Akt, and PI3K

The immunoreactivities of p-Akt, t-Akt, and PI3K were detected using immunohistochemistry. The results showed that paclitaxel reduced the percentage of both PI3K- and p-Akt-positive cells, whereas the number of both PI3K- and p-Akt-positive cells was increased after RES treatment (*P*<0.05). There was a significant increase between the groups P and R+P regarding the number of both PI3K- and p-Akt-positive cells. The number of positive cells can be reduced by the pretreatment of RES and LY294002 (*P*<0.05, Table 1). There were no statistically significant differences among the groups for t-Akt (*P*>0.05) (Figure 4).

Protein analysis

To investigate the potential mechanism of RES in the treatment of paclitaxel-induced neuropathic pain at protein level, the p-Akt, t-Akt, SIRT1, and PGC1 α proteins were measured by Western blot. As shown in Figure 5A-a, the expression of p-Akt in the corpus striatum of paclitaxel-treated group was significantly decreased compared to those in the control group (*P*<0.05), but significant increase was found in the samples treated with RES (*P*<0.05). Furthermore, the expression levels of p-Akt in the corpus striatum were suppressed by LY294002 (*P*<0.05). Nevertheless, the expression of t-Akt in the corpus striatum was not significantly changed. The expressions of Sirt1 and PGC1 α in corpus striatum (Figure 5A-b), SDH (Figure 5B), and DRG (Figure 5C) were significantly decreased in the paclitaxel-treated group compared to those in the control group (*P*<0.05). Compared to P+R group, the amount of SIRT1 and PGC1 α expression in corpus striatum, SDH, and DRG was suppressed by SIRT1 inhibitor (*P*<0.05).

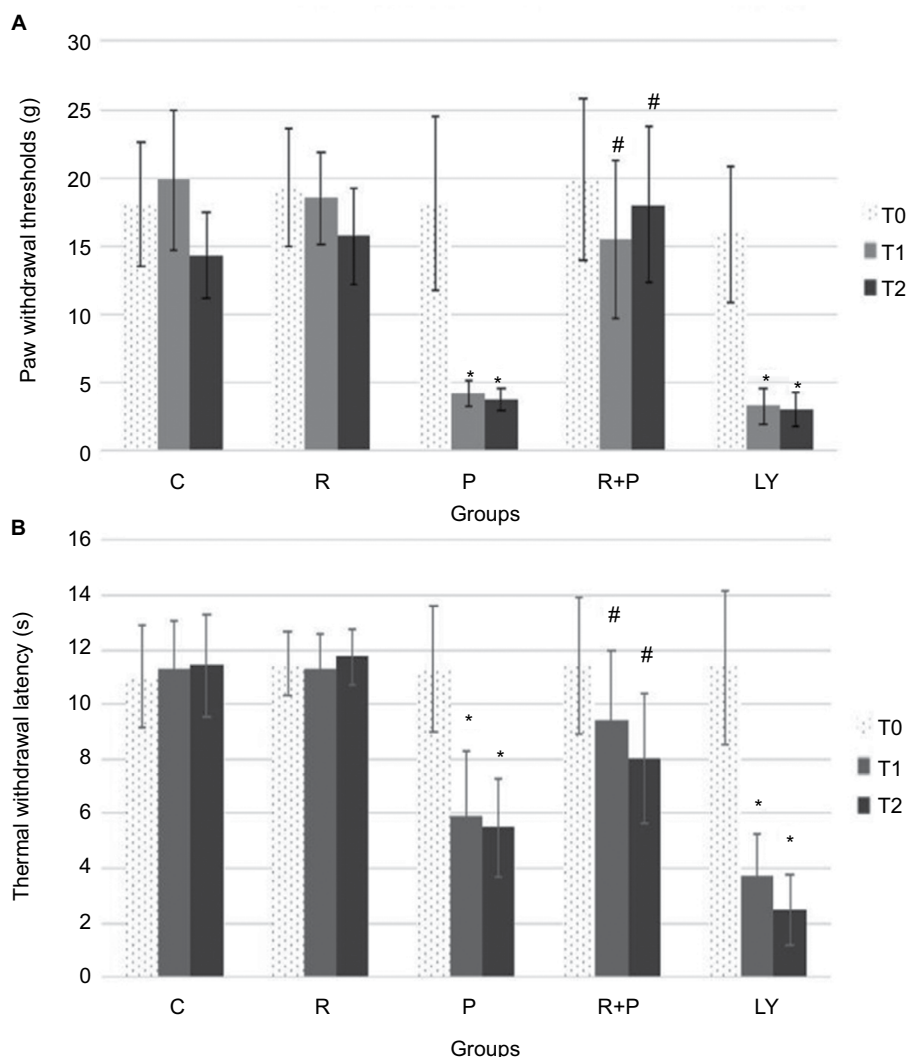


Figure 2 Paclitaxel-induced mechanical and heat hypersensitivity.

Notes: (A) Paw withdrawal mechanical threshold of five groups (ten for each) at T0, T1, and T2. * $P < 0.05$ compared to control animals, # $P < 0.05$ compared to paclitaxel-treated rats. (B) Thermal withdrawal latency of five groups (ten for each) at T0, T1, and T2. * $P < 0.05$ compared to control animals, # $P < 0.05$ compared to paclitaxel-treated rats.

Abbreviations: C, control group; R, resveratrol group; P, paclitaxel-treated group; R+P, resveratrol + paclitaxel-treated group; LY, LY294002 group.

TUNEL analysis

Compared to the control group, the rate of apoptosis in the corpus striatum, SDH, and DRG tissues in P group was significantly increased from 12%, 8%, and 11% to 44%, 49%, and 45%, but not significantly changed in R group (Table 2). Compared to group P, the number of apoptosis in group P+R was obvious reduced after RES intervention. However, after the addition of EX-527, the apoptotic rate increased significantly. Paclitaxel accelerates apoptosis in the corpus striatum, SDH, and DRG of paclitaxel-induced neuropathic rats; however, the number of apoptotic cells was decreased after RES intervention (Figure 6). The aforementioned findings further demonstrate that the symptoms of neuralgia

caused by paclitaxel may be related to apoptosis, which can be reduced by RES.

ELISA analysis

The expressions of IL-1 β in corpus striatum, SDH, and DRG are shown in Figure 6. The IL-1 β content of the P group was higher than that of the C group ($P < 0.05$), and that of the R group was lower than that of the P group ($P < 0.05$). Compared to the P+R group, the amount of IL-1 β expression was significantly increased in the E group ($P < 0.05$). In the three parts of corpus striatum, SDH, and DRG, the IL-10 content of the P group was lower than that of the group of control ($P < 0.05$), and that of the R group was higher than that of

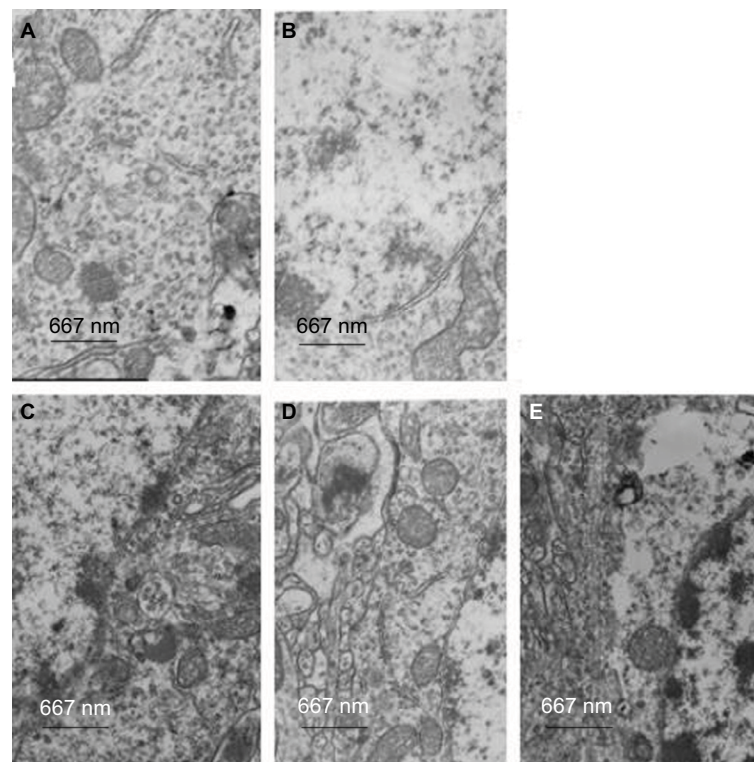


Figure 3 Mitochondrial histomorphology in the corpus striatum of five groups at day 14 by transmission electron microscopy.

Notes: (A) Control group (n=5); (B) resveratrol group (n=5); (C) paclitaxel-treated group (n=5); (D) resveratrol + paclitaxel-treated group (n=5); (E) LY294002 + resveratrol + paclitaxel-treated group (n=5).

Table 1 The number of positive cells of p-Akt, t-Akt, and PI3K in striatum determined by immunohistochemistry (%; n=5, $\bar{x} \pm s$)

Group	p-Akt	t-Akt	PI3K
C	26.3±1.5	33.0±3.0	26.3±3.1
P	16.7±2.1 [#]	30.7±1.5	12.2±2.1 [#]
R	36±1.7	32.3±1.3	34.7±3.2
P+R	19.3±2.0 [*]	32.3±2.0	20.7±2.1 [*]
LY + R+P	8.4±1.4 [*]	33.0±1.5	9.0±2.0 [*]

Note: Compared with C group, [#] $P < 0.05$; compared with P group, ^{*} $P < 0.05$; compared with P+R group, ^{*} $P < 0.05$.

Abbreviations: C, control group; R, resveratrol group; P, paclitaxel-treated group; R+P, resveratrol + paclitaxel-treated group; LY, LY294002 group; PI3K, phosphoinositide 3-kinase.

the P group ($P < 0.05$). Compared to the P+R group, the expression of IL-10 was decreased in the E group ($P < 0.05$) (Figure 7). In the three parts of corpus striatum, SDH, and DRC in rats with neuralgia induced by paclitaxel, the expression of IL-10 was opposite to IL-1 β . It is suggested that RES may improve the pain symptoms of paclitaxel neuralgia rats by increasing the expression of IL-10 and decreasing the expression of IL-1 β . MDA is a product of lipid peroxidation and an important indicator for detecting the degree of oxidative damage. In the corpus striatum, SDH, and DRG,

the MDA assay of P group was higher than that of the group of control ($P < 0.05$) (Figure 7), and that of the R group was lower than that of the P group ($P < 0.05$). Compared to the P+R group, the MDA assay was increased in the E group ($P < 0.05$). SOD is an antioxidant that eliminates harmful substances produced by organisms during metabolism. The assay of SOD in the corpus striatum, SDH, and DRG of P group was lower than that of the group of control ($P < 0.05$), and that of the R group was higher than that of the P group ($P < 0.05$). Compared to the P+R group, the SOD assay was decreased in the E group ($P < 0.05$) (Figure 7). The opposite assay results of SOD and MDA reveal that the nerve damage in rats with paclitaxel-induced neuropathic pain is closely related to oxidative stress.

Discussion

This study aimed to investigate the effect of RES on paclitaxel-induced neuropathic pain and explore the role of PI3K/Akt and SIRT1/PGC1 α signaling in it. Our findings suggest that paclitaxel-induced neuropathic painful peripheral neuropathies were associated with an abnormal incidence of swollen and vacuolated mitochondria

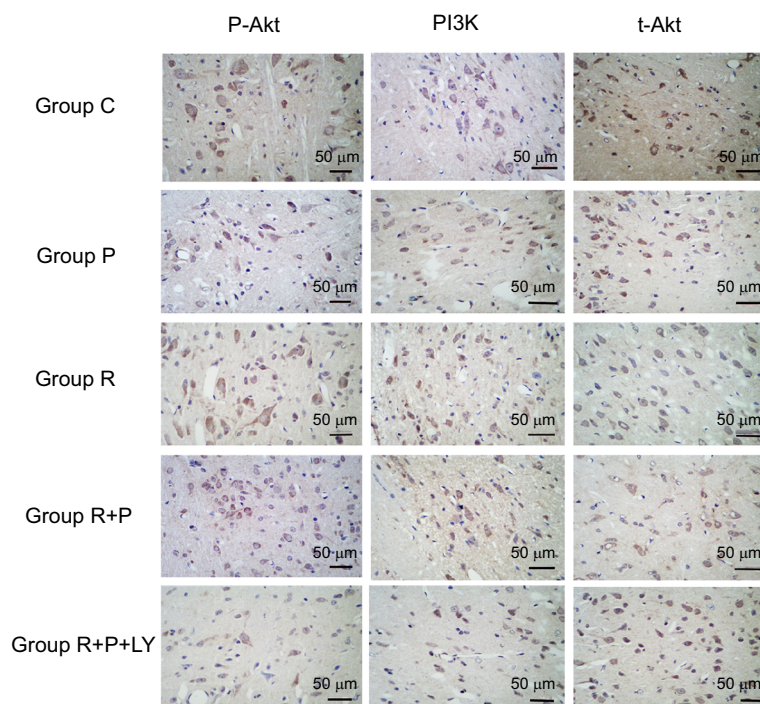


Figure 4 The expressions of p-Akt, PI3K, and t-Akt in five groups (five for each) were detected by immunohistochemistry.

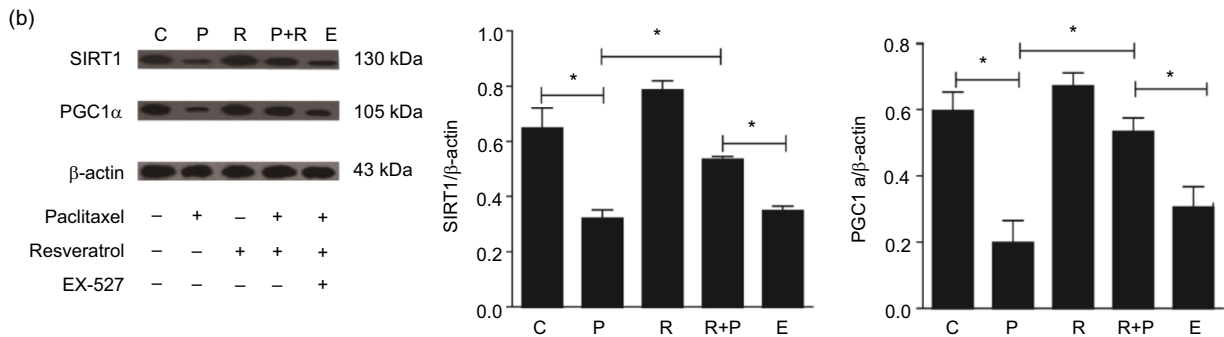
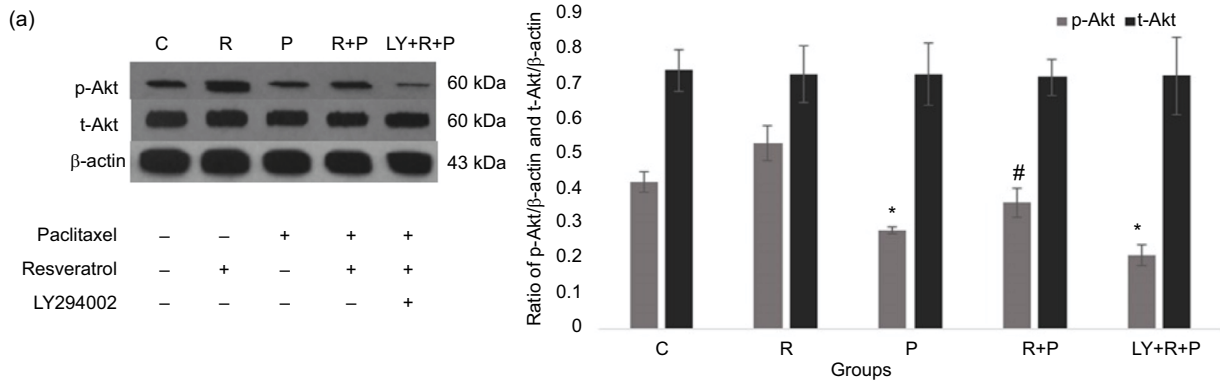
Abbreviations: C, control group; R, resveratrol group; P, paclitaxel-treated group; R+P, resveratrol + paclitaxel-treated group; R+P+LY, pretreated-resveratrol + pretreated-paclitaxel + LY294002; PI3K, phosphoinositide 3-kinase.

on corpus striatum, and also reduced the expression of p-Akt. RES alleviated the paclitaxel-induced neuropathic pain through activation of PI3K/Akt and SIRT1/PGC1 α signaling. These results reveal the critical role of PI3K/Akt and SIRT1/PGC1 α signaling in paclitaxel-induced neuropathic pain.

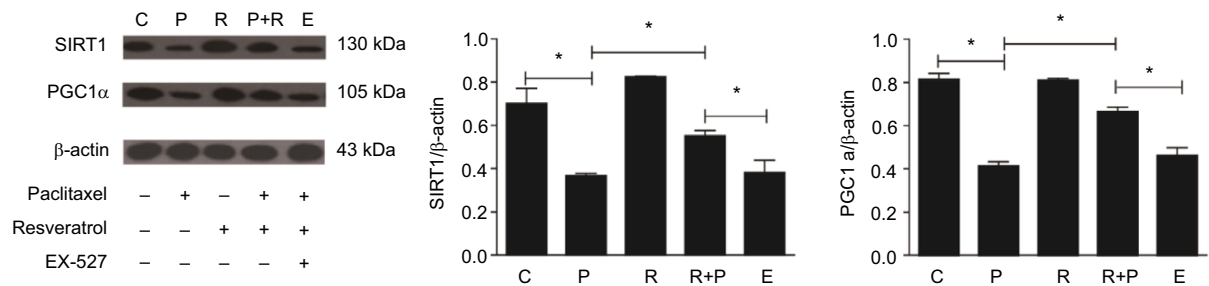
Manifestation of mitochondrial swelling and vacuolation in peripheral nerve axons confirmed the paclitaxel-induced mitotoxicity, which suggests that these drugs cause a chronic sensory axonal energy deficiency that is the primary cause of the neuropathies' symptoms.^{5,13} Mitochondrial function is mainly involved in the oxidative phosphorylation and breathing in the process of electron transfer; it could provide energy for the body activities and also stimulate the production of ROS simultaneously. There is evidence that excessive ROS can induce mitochondrial function damage and reduce the production of ATP in paclitaxel-treated animals at both the early and late time points.¹³ Another point here is that paclitaxel leads to significant deficits in complex I-mediated and complex II-mediated respiration in sensory axons.²⁶ The results of the present study reported that paclitaxel-induced neuropathic pain was associated with mitochondrial damages.

It is widely recognized that RES is a compound with strong antioxidant activity, which might directly inhibit O₂ oxidation and prevent ROS production. Meanwhile, RES is identified as a potent activator of SIRT1.²³ A study by Khan RS demonstrated that RES reduces oxidative stress and promotes mitochondrial function in neuronal cells through activation of SIRT1.²¹ This suggests that RES has the potential to preserve neurons in other neurodegenerative diseases through mediating neuroprotective effects. SIRT1 and its substrate, PGC1 α , regulate energy metabolism through the mitochondria.³² However, our study of the SIRT1/PGC1 α signaling pathway was related to the study of the regulation of energy metabolism by mitochondria. Our findings show that the SIRT1/PGC1 α signaling pathway can be activated by RES and can be inhibited by EX-527. Meanwhile, RES can reduce apoptosis, inhibit inflammation, maintain redox balance, and protect mitochondrial function. Also, many signaling pathways may be activated by RES, such as mitochondria-mediated and Bcl-2 proteins alteration.²⁷ It has been reported that PI3K/Akt signaling may play a critical role in nociceptor sensitivity during neuropathic pain. There are a lot of evidences to prove that the PI3K/Akt cascade participates in many cell functions including metabolism,

A



B



C

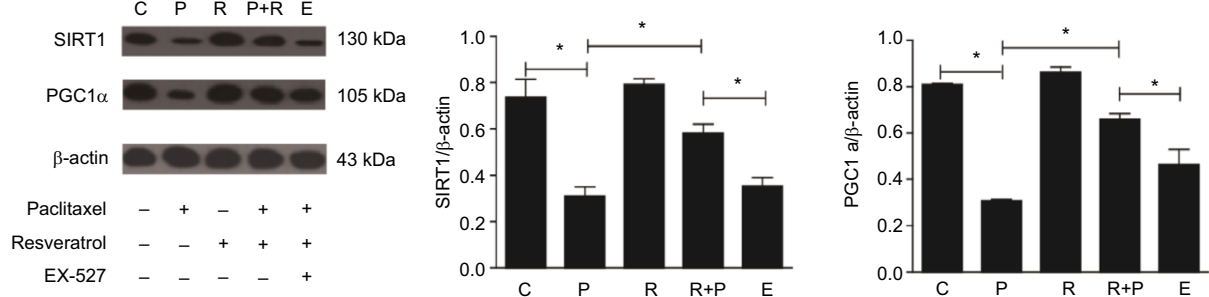


Figure 5 Protein levels of t-Akt and p-Akt in corpus striatum (A-a). Three rats in each group. * $P < 0.05$ compared to control animals, # $P < 0.05$ compared to paclitaxel-treated rats. Protein levels of SIRT1 and PGC1α in corpus striatum (A, B). Protein levels of SIRT1 and PGC1α in spinal dorsal horn (B). Protein levels of SIRT1 and PGC1α in spinal dorsal horns (C). Protein levels of SIRT1 and PGC1α in dorsal root ganglions (D). Paclitaxel reduced the expression levels of SIRT1 and PGC1α (* $P < 0.05$), while resveratrol increased the expression of SIRT1 and PGC1α (* $P < 0.05$); the protein levels of SIRT1 and PGC1α were suppressed by EX527 (* $P < 0.05$).

Abbreviations: C, control group; R, resveratrol group; P, paclitaxel-treated group; R+P, resveratrol + paclitaxel-treated group; R+P+LY, pretreated-resveratrol + pretreated-paclitaxel + LY294002; E, pretreated-resveratrol + pretreated-paclitaxel + EX-527 group SIRT1, sirtuin 1.

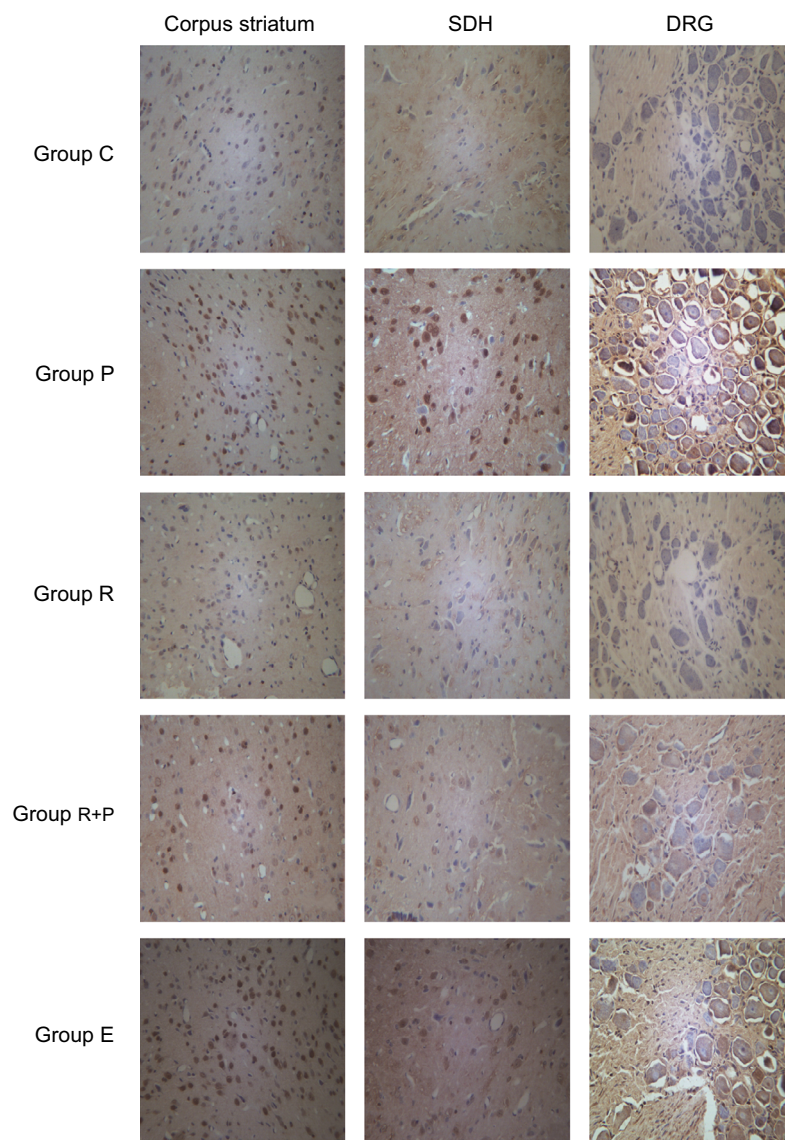
Table 2 The apoptotic rate of corpus striatum, SDH, and DRG

Groups	Apoptotic rate (%)		
	Corpus striatum	SDH	DRG
C	12%	8%	11%
P	44%	49%	45%
R	7%	7%	9%
R+P	31%	33%	28%
E	42%	45%	41%

Notes: Group C was the control rats; Group P was paclitaxel-treated rats; Group R received RES treatment; Group R+P was treated with paclitaxel with the pretreatment of RES; Group E underwent paclitaxel treatment with the pretreatment of RES and EX-527.

Abbreviations: C, control group; R, resveratrol group; P, paclitaxel-treated group; R+P, resveratrol + paclitaxel-treated group; DRG, dorsal root ganglions; RES, resveratrol; SDH, spinal dorsal horns; E, pretreated-resveratrol + pretreated-paclitaxel + EX-527 group.

proliferation, or growth.^{1,14} Therefore, the dysregulation of this cascade can lead to a variety of conditions, including cancer, diabetes, and neurologic diseases.^{17,25} Findings of the present study are consistent with the previous studies, which reported that the inhibition of PI3K dramatically alleviates inflammatory and neuropathic pain.^{19,20,30} Several studies have demonstrated that RES can reverse mitochondrial damage against oxidative stress-induced neuronal death through the activation of PI3K/Akt signaling pathway.^{2,24} In vivo researches reported that PI3K inhibitor, LY29400, can significantly reduce the level of spinal microglia in animal model of bone cancer pain.²⁰

**Figure 6** Apoptosis in the corpus striatum, SDH, and DRG of rats with neuralgia induced by paclitaxel.

Notes: Compared to the control, the number of apoptosis in group P was increased, and group R has no significant change in apoptosis. In the resveratrol treatment group P+R, the apoptosis was decreased compared to group P. In the inhibitor treatment group E, the apoptosis was increased compared to group P.

Abbreviations: C, control group; R, resveratrol group; P, paclitaxel-treated group; R+P, resveratrol + paclitaxel-treated group; DRG, dorsal root ganglions; SDH, spinal dorsal horns; E, pretreated-resveratrol + pretreated-paclitaxel + EX-527 group.

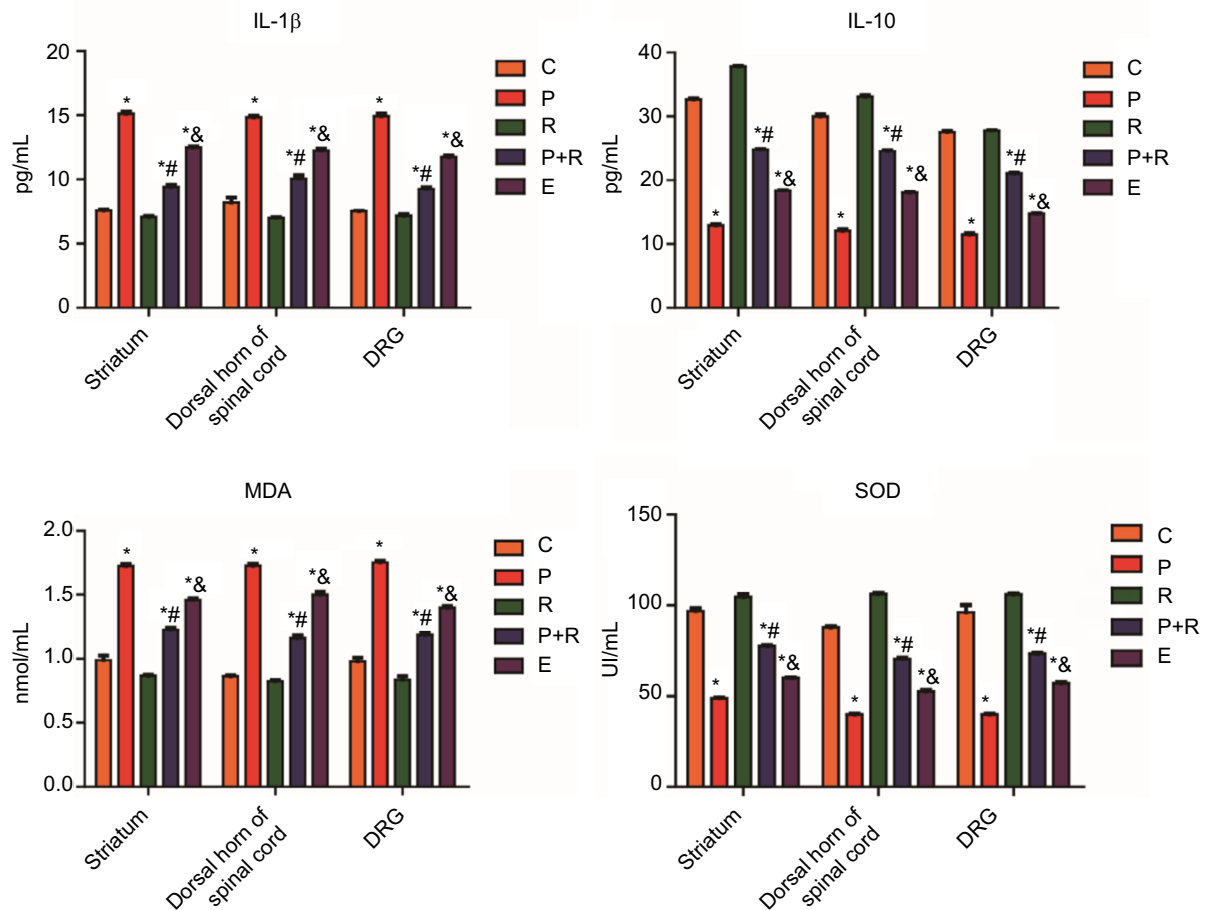


Figure 7 The expression of IL-1 β , IL-10, MDA, and SOD in the corpus striatum, SDH, and DRG tissues.

Notes: Five rats in each group. * $P < 0.05$ compared to control animals, # $P < 0.05$ compared to paclitaxel-treated rats, & $P < 0.05$ compared to rats treated with paclitaxel with the pretreatment of resveratrol.

Abbreviations: C, control group; R, resveratrol group; P, paclitaxel-treated group; R+P, resveratrol + paclitaxel-treated group; DRG, dorsal root ganglions; MDA, malondialdehyde; SDH, spinal dorsal horns; SOD, superoxide dismutase.

Conclusion

The findings suggest that RES can prevent paclitaxel-induced neuropathic pain by activating the PI3K/Akt signaling pathway, which protects the mitochondrial function of the corpus striatum. We further demonstrated that in a rat model of paclitaxel-induced neuropathic pain, RES can improve the symptoms of neuralgia by activating the SIRT1/PGC1 α signaling pathway because it reduces apoptosis, inhibits inflammation, and relieves oxidative stress by regulating the SIRT1/PGC1 α signaling pathway.

Acknowledgment

This work was supported by National Natural Science Foundation of China (no. 81371231).

Disclosure

The authors report no conflicts of interest in this work.

References

- Bareiss SK, Dugan E, Brewer KL. PI3K mediated activation of GSK-3 β reduces At-level primary afferent growth responses associated with excitotoxic spinal cord injury dysesthesias. *Mol Pain*. 2015;11:35.
- Bellaver B, Bobermin LD, Souza DG, et al. Signaling mechanisms underlying the glioprotective effects of resveratrol against mitochondrial dysfunction. *Biochim Biophys Acta*. 2016;1862(9):1827–1838.
- Ceber M, Sener U, Mihmanli A, Kilic U, Topcu B, Karakas M. The relationship between changes in the expression of growth associated protein-43 and functional recovery of the injured inferior alveolar nerve following transection without repair in adult rats. *J Craniomaxillofac Surg*. 2015;43(9):1906–1913.
- Chaplan SR, Bach FW, Pogrel JW, Chung JM, Yaksh TL. Quantitative assessment of tactile allodynia in the rat paw. *J Neurosci Methods*. 1994;53(1):55–63.
- Chen MM, Yin ZQ, Zhang LY, Liao H. Quercetin promotes neurite growth through enhancing intracellular cAMP level and GAP-43 expression. *Chin J Nat Med*. 2015;13(9):667–672.
- Colombel JF, Rutgeerts P, Reinisch W, et al. Early mucosal healing with infliximab is associated with improved long-term clinical outcomes in ulcerative colitis. *Gastroenterology*. 2011;141(4):1194–1201.
- Das S, Das DK. Anti-inflammatory responses of resveratrol. *Inflamm Allergy Drug Targets*. 2007;6(3):168–173.

8. Dixon WJ. Efficient analysis of experimental observations. *Annu Rev Pharmacol Toxicol.* 1980;20(1):441–462.
9. Durán N, Martínez DS, Silveira CP, et al. Graphene oxide: a carrier for pharmaceuticals and a scaffold for cell interactions. *Curr Top Med Chem.* 2015;15(4):309–327.
10. Feito MJ, Vila M, Matesanz MC, et al. In vitro evaluation of graphene oxide nanosheets on immune function. *J Colloid Interface Sci.* 2014;432:221–228.
11. Fu SY, Gordon T. The cellular and molecular basis of peripheral nerve regeneration. *Mol Neurobiol.* 1997;14(1–2):67–116.
12. Furuse M, Fujita K, Hiiragi T, Fujimoto K, Tsukita S. Claudin-1 and -2: novel integral membrane proteins localizing at tight junctions with no sequence similarity to occludin. *J Cell Biol.* 1998;141(7):1539–1550.
13. Gordon T, Tetzlaff W. Regeneration-associated genes decline in chronically injured rat sciatic motoneurons. *Eur J Neurosci.* 2015;42(10):2783–2791.
14. Gordon T, Tyreman N, Raji MA. The basis for diminished functional recovery after delayed peripheral nerve repair. *J Neurosci.* 2011;31(14):5325–5334.
15. Gordon T, You S, Cassar SL, Tetzlaff W. Reduced expression of regeneration associated genes in chronically axotomized facial motoneurons. *Exp Neurol.* 2015;264:26–32.
16. Guo X, Mei N. Assessment of the toxic potential of graphene family nanomaterials. *J Food Drug Anal.* 2014;22(1):105–115.
17. Hemmings BA, Restuccia DF. PI3K-PKB/Akt pathway. *Cold Spring Harb Perspect Biol.* 2012;4(9):a011189.
18. Ishige K, Schubert D, Sagara Y. Flavonoids protect neuronal cells from oxidative stress by three distinct mechanisms. *Free Radic Biol Med.* 2001;30(4):433–446.
19. Jiang SP, Zhang ZD, Kang LM, Wang QH, Zhang L, Chen HP. Celecoxib reverts oxaliplatin-induced neuropathic pain through inhibiting PI3K/Akt2 pathway in the mouse dorsal root ganglion. *Exp Neurol.* 2016;275 Pt 1:11–16.
20. Jin D, Yang JP, Hu JH, Wang LN, Zuo JL. MCP-1 stimulates spinal microglia via PI3K/Akt pathway in bone cancer pain. *Brain Res.* 2015;1599:158–167.
21. Khan RS, Fonseca-Kelly Z, Callinan C, Zuo L, Sachdeva MM, Shindler KS. SIRT1 activating compounds reduce oxidative stress and prevent cell death in neuronal cells. *Front Cell Neurosci.* 2012;6:63.
22. Li B, Luo X, Li T, et al. Effects of constant flickering light on refractive status, 5-HT and 5-HT2A receptor in guinea pigs. *PLoS One.* 2016;11(12):e0167902.
23. Lin CH, Lin CC, Ting WJ, et al. Resveratrol enhanced FOXO3 phosphorylation via synergetic activation of SIRT1 and PI3K/Akt signaling to improve the effects of exercise in elderly rat hearts. *Age.* 2014;36(5):9705.
24. Liu X, Wang J, Dong F, Li H, Hou Y. Induced differentiation of human gingival fibroblasts into VSMC-like cells. *Differentiation.* 2017;95:1–9.
25. Liu X, Wang J, Dong F, et al. Cytocompatibility and biologic characteristics of synthetic scaffold materials of rabbit acellular vascular matrix combining with human-like collagen I. *J Biomater Appl.* 2017;32(4):463–471.
26. Onodera N, Kakehata A, Araki I. Differential expression of GAP-43 protein in the rostral brain neurons of early chick embryos. *Tohoku J Exp Med.* 2013;231(4):293–298.
27. Park JW, Choi YJ, Suh SI, et al. Bcl-2 overexpression attenuates resveratrol-induced apoptosis in U937 cells by inhibition of caspase-3 activity. *Carcinogenesis.* 2001;22(10):1633–1639.
28. Reinisch W, Sandborn WJ, Hommes DW, et al. Adalimumab for induction of clinical remission in moderately to severely active ulcerative colitis: results of a randomised controlled trial. *Gut.* 2011;60(6):780–787.
29. Sanna MD, Ghelardini C, Galeotti N. HuD-mediated distinct BDNF regulatory pathways promote regeneration after nerve injury. *Brain Res.* 2017;1659:55–63.
30. Saponaro C, Cianciulli A, Calvello R, Dragone T, Iacobazzi F, Panaro MA. The PI3K/Akt pathway is required for LPS activation of microglial cells. *Immunopharmacol Immunotoxicol.* 2012;34(5):858–865.
31. Stefano MED, Toni F, Orazi VD, Ortensi A, Tata AM. Therapeutic approaches enhancing peripheral nerve regeneration. *Adv Biosci Biotechnol.* 2013;04(06):53–60.
32. Tang BL. SIRT1 and the mitochondria. *Mol Cells.* 2016;39(2):87–95.
33. Tsukita S, Furuse M, Itoh M. Multifunctional strands in tight junctions. *Nat Rev Mol Cell Biol.* 2001;2(4):285–293.
34. Yin Q, Lu FF, Zhao Y, et al. Resveratrol facilitates pain attenuation in a rat model of neuropathic pain through the activation of spinal SIRT1. *Reg Anesth Pain Med.* 2013;38(2):93–99.

Journal of Pain Research

Publish your work in this journal

The Journal of Pain Research is an international, peer reviewed, open access, online journal that welcomes laboratory and clinical findings in the fields of pain research and the prevention and management of pain. Original research, reviews, symposium reports, hypothesis formation and commentaries are all considered for publication.

Submit your manuscript here: <https://www.dovepress.com/journal-of-pain-research-journal>

Dovepress

The manuscript management system is completely online and includes a very quick and fair peer-review system, which is all easy to use. Visit <http://www.dovepress.com/testimonials.php> to read real quotes from published authors.